International Journal of Mass Spectrometry 505 (2024) 117313

Contents lists available at ScienceDirect

International Journal of Mass Spectrometry

journal homepage: www.elsevier.com/locate/ijms

Structures, energies and vibrational frequencies of the X and A states of haloacetylene cations, $HCCX^+$ (X = F, Cl, Br, I)

Andrew S. Durden [a], Marco Caricato [b], H. Bernhard Schlegel [a,*]

[a] Department of Chemistry, Wayne State University, Detroit, MI, 48202, USA
[b] Department of Chemistry, University of Kansas, Lawrence, KS, 66045, USA

ARTICLE INFO

Keywords:
Haloacetylene
Ionization
Excited cation
Molecular structure
Vibrational frequencies
EOMCCSD-IP

ABSTRACT

Modeling charge migration resulting from the coherent superposition of cation ground and excited states requires information about the potential energy surfaces of the relevant cation states. Since these states are often of the same electronic symmetry as the ground state of the cation, conventional single reference methods such as coupled cluster cannot be used for the excited states. The EOMCCSD-IP (equation of motion coupled cluster with single and double excitations and ionization) is a convenient and reliable "black-box" method that can be used for the ground and excited states of cations, yielding results of CCSD (coupled cluster with singles and double excitation) quality. Charge migration in haloacetylene cations arises from the superposition of the X and A states of $HCCX^+$ (X = F, Cl, Br and I). The geometries, ionization potentials and vibrational frequencies have been calculated by CCSD/cc-pVTZ for neutral HCCX and the X state of $HCCX^+$ and by EOM CCSD-IP/cc-pVTZ for the X and A states of $HCCX^+$. The results agree very well with each other and with experiment. The very good agreement between CCSD and EOMCCSD-IP for the X states demonstrates that EOMCCSD-IP is a suitable method for calculating the structure and properties of ground and excited states for the HCCX cations.

1. Introduction

The coherent superposition of cation states can result in charge migration on the natural time scale of electron dynamics in molecules [1–8]. Strong field ionization can produce suitable coherent superpositions of the ground and excited states of a cation, but the resulting charge migration may be challenging to observe experimentally. Modeling the decoherence of charge migration requires information about the potential energy surfaces of the relevant states of the cation. Some of this information can be gleaned from photoelectron spectra [9], but these spectra are often dense and difficult to analyze. Computational methods can provide structures and vibrational frequencies of the ground and excited states of cations to help analyze photoelectron spectra and to simulate electron dynamics in coherent superpositions of cation states. In the present computational study, we examine the ground and excited states of a series of haloacetylene cations, $HCCX^+$ (X = F, Cl, Br, I), in preparation for future studies on the formation of coherent superpositions and the simulation of charge migration in these systems.

Charge migration in $HCCI^+$ has been studied extensively, both experimentally and computationally [4,10–16]. Strong field ionization of HCCI produces a coherent superposition of the X and A states of $HCCI^+$ [4]. This results in charge migration between the CC triple bond and the iodine with a period of 1.87 fs. The coherent superposition and charge migration decay in 15–20 fs because the vibrational wavepackets on the X and A potential energy surfaces move in opposite directions [12–15]. Charge migration has also been studied in a number of other systems, including some closely related molecules, HCCBr, $H(CC)_nBr$ and $H(CC)_nI$ cations [17–19], but not in $HCCCl^+$ and $HCCF^+$.

One of the challenges for calculating the electronic structure of HCCX cations is that the X and A states have the same electronic state symmetry. Consequently, calculations of the A state with conventional density functional methods and single reference correlated wavefunctions such as coupled clusters (CC) would collapse to the X state. CASSCF (complete active space self-consistent field) and CASPT2 (CASSCF with second order perturbation theory) are appropriate methods but the active space must be carefully selected for each individual molecule. It would be highly desirable to have a straight-forward, "black-box" method that can treat the ground state and excited states of radical cations with the same accuracy and that does not need to be customized for each molecule. EOMCCSD-IP[20–23] (equation of motion coupled cluster with single and double excitations and ionization) is

* Corresponding author.
E-mail address: hbs@chem.wayne.edu (H.B. Schlegel).

https://doi.org/10.1016/j.ijms.2024.117313
Received 23 June 2024; Received in revised form 30 July 2024; Accepted 1 August 2024
Available online 2 August 2024
1387-3806/Published by Elsevier B.V.

potentially such a "black-box" method that is similar in accuracy to calculations with CCSD (CC with single and double excitation) and is more efficient than CCSD for radical cations. In this formalism, calculations of open shell cations start with a CCSD calculation of the closed shell neutral molecule. The wavefunctions for the ground and excited states of the radical cation are then generated using an equation of motion approach involving single ionization and single excitations of the coupled cluster wavefunction for the neutral molecule. For reviews of coupled cluster methods such as CCSD, EOMCCSD and EOMCCSD-IP see Refs. [24–26].

In a previous study, we investigated the angular dependence of strong field ionization in HCCX (X = F, Cl, Br, I) [27]. In recent work we simulated charge migration and decoherence in $HCCI^+$ with time-dependent configuration interaction (TDCI) using geometries and vibrational frequencies for the X and A states of HCCI cation available in the literature [15,16]. In the present work we have calculated the structures, ionization potentials and vibrational frequencies of HCCX cations in the X and A states with CCSD and EOMCCSD-IP using a cc-pVTZ basis set. The calculated data will be used in future simulations of charge migration and decoherence in these systems.

2. Methods

Calculations of HCCX (X = F, Cl, Br, I) were carried out with the development version of the Gaussian software package [28] and employed the cc-pVTZ basis set [29–32]. Ionization energies were calculated with coupled cluster methods (CCSD, EOMCCSD-IP) and electron propagator theory [33] (EPT). CCSD was used to calculate optimized geometries of neutral HCCX and the X state of HCCX cations. EOMCCSD-IP energy calculations, recently added to Gaussian by one of the authors (MC), were used for the X and A states of the HCCX cations. Geometries were optimized with the Fletcher-Powell approach [34] using numerical first derivatives and frequencies were calculated using double numerical differentiation of the energy. Spin-orbit coupling and vibrational anharmonicity corrections were not included in the present calculation.

3. Results and discussion

The structures of neutral HCCX are well-established experimentally (Table 1). The CCSD/cc-pVTZ optimized geometries are in very good agreement with experiment [35–38] and recent high-level calculations [4,39]. The shortening of the CC bond in HCCF compared to the other HCCX is a result of reduced interactions between the CC triple bond and the very electronegative fluorine.

The highest occupied molecular orbitals of HCCX are shown in Fig. 1 and the geometries of the ground state of the haloacetylene cations (X states) are listed in Table 2. The X states of the HCCX cations are generated by removing an electron from the π* orbital, which has a node between the CC π orbital and the π-type lone pair on X. As a result, the CX bond is shorter than in the neutral while the CC bond is longer. The calculated bond lengths and their values as a function of the halogen are in very good agreement with the estimated experimental structures and trends. The changes in bond length on ionization have been approximated by Heilbronner [40] based on the changes in spacing and

Table 1
Geometries of linear HCCX (Å).

	HCCF	HCCCl	HCCBr	HCCI
CCSD[a]				
R(CX)	1.278	1.648	1.793	1.997
R(CC)	1.196	1.202	1.203	1.206
R(CH)	1.059	1.060	1.061	1.062
Experiment[b]				
R(CX)	1.276	1.638	1.792	1.989
R(CC)	1.196	1.203	1.204	1.206
R(CH)	1.060	1.055	1.055	1.056

[a] present calculations with the cc-pVTZ basis set.
[b] HCCF [35], HCCCl [36], HCCBr [37], HCCI [38].

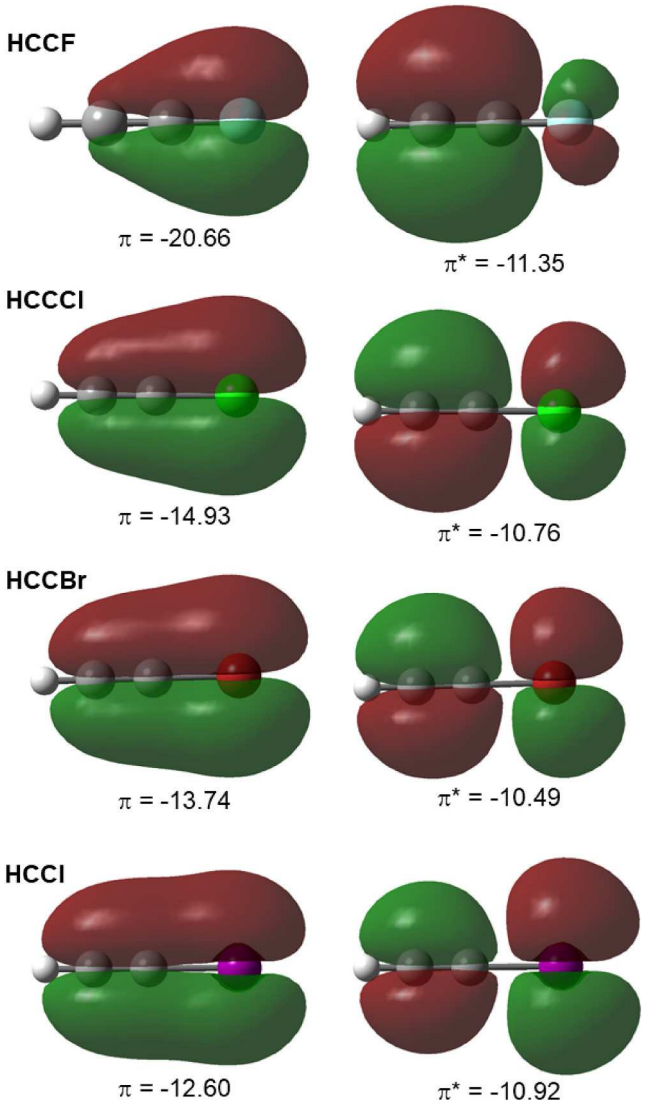

Fig. 1. Highest occupied π and π* molecular orbitals of HCCX (X = F, Cl, Br, I) and their orbital energies in eV.

Table 2
Geometries of the X States of linear $HCCX^+$ (Å).

	$HCCF^+$	$HCCCl^+$	$HCCBr^+$	$HCCI^+$
CCSD[a]				
R(CX)	1.218	1.577	1.723	1.929
R(CC)	1.243	1.243	1.238	1.228
R(CH)	1.076	1.074	1.072	1.071
EOMCCSD-IP[a]				
R(CX)	1.216	1.577	1.725	1.934
R(CC)	1.236	1.236	1.231	1.222
R(CH)	1.077	1.074	1.073	1.071
Experiment[b]				
R(CX)	(1.213)	1.582[c] (1.581)		1.89[d] (1.919)
R(CC)	(1.249)	(1.228)		(1.231)
R(CH)	(1.080)	(1.070)		(1.067)

[a] present calculations with the cc-pVTZ basis set.
[b] The numbers in parenthesis are geometry differences obtained by Heilbronner [40] added to the geometries of the neutral HCCX in Table 1.
[c] Ref [41].
[d] Ref [42].

Table 3
Geometries of the A States of linear $HCCX^+$ (Å).

	HCCF $^+$ [b]	$HCCCl^+$	$HCCBr^+$	$HCCI^+$
EOMCCSD-IP[a]				
R(CX)	1.486	1.771	1.903	2.096
R(CC)	1.192	1.210	1.218	1.233
R(CH)	1.071	1.071	1.071	1.072
Experiment[c]				
R(CX)		1.745[d] (1.777)	(1.947)	2.09[e] (2.149)
R(CC)		(1.231)	(1.235)	(1.217)
R(CH)		(1.066)	(1.067)	(1.062)

[a] present calculations with the cc-pVTZ basis set.
[b] The linear structure for the A state of HCCF $^+$ has 2 imaginary frequencies; the *trans* bent structure is a minimum: R(CF) = 1.502 Å, R(CC) = 1.217 Å, R(CH) = 1.074 Å, ∠CCF = 145.9, ∠CCH = 162.0.
[c] The numbers in parenthesis are geometry differences obtained Heilbronner [40] added to the geometries of the neutral HCCX in Table 1.
[d] Ref [41].
[e] Ref [42].

intensities of the fine structure in photoelectron spectra. These differences are added to the bond length in Table 1 to provide semi-quantitative estimates of the geometries for the X and A states of the cations. Maier and coworkers [41,42] measured the rotational constants for the X and A states of HCCX and DCCX cations (X = Cl, I) and used the R(CH) and R(CC) distances estimated by Heilbronner [40] to obtain R (CX) bond lengths for the X and A states of HCCX. The very good agreement between the CCSD and EOMCCSD-IP optimized geometries of the X states indicates that EOMCCSD-IP should be very suitable for the excited A states of the cations.

The first excited states of $HCCX^+$ (A states) are generated by removing an electron from the second highest occupied orbital, a π orbital with no node between the CC π orbital and the π-type lone pair on the halogen (see Fig. 1). Because the A states of the HCCX cations have the same electronic symmetry as the X states, CCSD calculations would collapse to the lower energy X state. To avoid this problem, the A states have been calculated with the EOMCCSD-IP method, which involves ionization and excitation of the CCSD wavefunction of the neutral molecule. Since the A state is formed by removing an electron from a π bonding orbital, both the CC and CX bonds are longer than in the neutral HCCX. HCCF, however, is a special case. The optimized linear geometry of HCCF has a pair of imaginary frequencies (see below). Further optimization yields a *trans*-bent geometry. In contrast to the other haloacetylenes, the fluorine lone pair orbitals in HCCF are significantly lower in energy than the CC π orbital. As can be seen in Fig. 1, the HCCF π orbital (−20.66 eV) is dominated by the fluorine lone pair. Furthermore, it is comparable in energy to the highest σ bonding orbital (−19.68 eV). Ionizing from the π bonding orbital yields a configuration that is slightly lower in energy than the configuration formed by ionizing from the highest σ orbital. Bending the CCF and CCH angles to allow these two configurations to interact thereby stabilizing the bent structure for the A state.

The difference in geometry between X and A states is a key factor in the rate of decay of a coherent superposition of the X and A states. This has been studied in detail for HCCI [4,10–16]. The largest changes are in the R(CX) bond lengths (0.194 Å, 0.178 Å and 0.162 Å for HCCCl, HCCBr and HCCI, respectively). The greater calculated change in R(CCl) compared to R(CI) suggests that decoherence could be somewhat faster for HCCCl than for HCCI.

The ionization potentials (IP) are listed in Table 4 The experimental adiabatic IP's for HCCCl, HCCBr and HCCI cations are for the lower energy J = 3/2 spin-orbit states. The calculated vertical IP's are obtained from the electronic energy difference at the geometry of the neutral molecule. Electron propagator theory [33] (EPT) provides an efficient way to compute vertical IP's that is comparable to 4th order many body perturbation theory and yields values within about 0.2 eV of the

Table 4
Ionization potentials and excitation energies (eV).

	HCCF[a]	HCCCl	HCCBr	HCCI
Vertical IP for X state				
EPT	11.523	10.775	10.442	9.840
CCSD	11.244	10.606	10.338	9.831
EOMCCSD-IP	11.482	10.781	10.460	9.887
Adiabatic IP for X state				
CCSD	11.005	10.422	10.190	9.744
EOMCCSD-IP	11.264	10.618	10.340	9.815
Experiment[a]	11.26	10.58	10.31	9.71
Vertical IP for A state				
EPT	18.264	13.976	13.056	12.127
EOMCCSD-IP	18.107	14.107	13.141	12.168
Adiabatic IP for A state				
EOMCCSD-IP	17.206[b]	13.887	12.971	12.018
Experiment[a]	18.0[c]	13.87	12.86	11.87
X → A Excitation				
EOMCCSD-IP	5.943[b]	3.269	2.631	2.203
Experiment [43]		3.291	2.548	2.154

[a] HCCF [44], HCCCl [43], HCCBr [43], HCCI [43].
[b] Linear; for *trans* bent structure, IP = 17.174 eV and X → A excitation = 5.910 eV.
[c] Vertical.

experimental adiabatic IP's. The CCSD and EOMCCSD-IP vertical IP's are also in very good agreement with the experiment. The CCSD values are lower than EOMCCSD-IP because the CCSD wavefunction is somewhat more flexible. The adiabatic IP's are calculated as the enthalpy difference at 0 K between the ion and the neutral, each at their respective minimum energy geometries. Relaxation of the ion structures to their equilibrium geometries lowers the energies by approximately 0.2 eV. The CCSD and EOMCCSD-IP calculated adiabatic IP's are within about 0.2 eV of the experimental adiabatic IP's. As noted above, the A state of HCCF is a special case. Relaxation of the linear geometry lowers the energy by 0.90 eV. Further relaxation to the bent structure (see footnote in Table 3) lowers the energy by an additional 0.032 eV and yields an adiabatic IP of 17.174 eV.

The frequency for charge migration in HCCX cations depends on the energy difference between the X and A states. Accurate experimental energy differences between X and A cation states in their ground vibrational state have been obtained from analysis of the A to X emission spectra. The EOMCCSD-IP calculations are in very good agreement, with differences of −0.016 to 0.087 eV.

The vibrational frequencies for neutral HCCX are listed in Table 5. The calculated harmonic frequencies differ from the observed frequencies by about 5 %, primarily because of vibrational anharmonicity. As X is changed from F to Cl, Br and I, the calculated frequencies reproduce the trends in the observed frequencies for each of the normal modes. The good agreement between the calculations and experiment suggests that the CCSD/cc-pVTZ method should be a satisfactory level of theory for calculating the vibrational frequencies for the cations.

Table 5
Vibrational frequencies of HCCX (cm^{-1}).

	HCCF	HCCCl	HCCBr	HCCI
CCSD				
ν_1 σ	3520	3503	3500	3492
ν_2 σ	2331	2206	2183	2156
ν_3 σ	1092	757	614	529
ν_4 π	615	647	655	666
ν_5 π	402	345	314	278
Experiment[a]				
ν_1 σ	3351	3340	3325	3327
ν_2 σ	2232	2110	2085	2063
ν_3 σ	1063	756	618	516
ν_4 π	584	604	618	630
ν_5 π	367	326	295	260

[a] HCCF [35], HCCCl [45], HCCBr [46], HCCI [47].

Table 6
Vibrational frequencies of the X state of $HCCX^+$ (cm^{-1}).

	$HCCF^+$	$HCCCl^+$	$HCCBr^+$	$HCCI^+$
CCSD				
ν_1 σ	3352	3373	3385	3405
ν_2 σ	2263	2081	2042	2015
ν_3 σ	1172	835	677	584
ν_4 π	578	599	623	675
ν_5 π	343	341	293	256
EOMCCSD-IP				
ν_1 σ	3349	3370	3384	3406
ν_2 σ	2289	2096	2061	2047
ν_3 σ	1187	841	681	582
ν_4 π	609	622	648	684
ν_5 π	365	345	311	265
Experiment[a]				
ν_1 σ		3249	3280	3258
ν_2 σ		1984	1931	1805
ν_3 σ		838	673	578
ν_4 π		636	618	542
ν_5 π		346	273	237

[a] HCCCl [49], HCCBr [46], HCCI [46].

Table 7
Vibrational frequencies of the A state of $HCCX^+$ (cm^{-1}).

	$HCCF^{+a}$	$HCCCl^+$	$HCCBr^+$	$HCCI^+$
EOMCCSD-IP				
ν_1 σ	3421	3414	3409	3389
ν_2 σ	2245	2183	2163	2105
ν_3 σ	766	622	517	449
ν_4 π	722	718	706	678
ν_5 π	151 *i*	245	248	249
Experiment[b]				
ν_1 σ		3249		
ν_2 σ		2064	2051	1822
ν_3 σ		596	492	407
ν_4 π			629	612
ν_5 π			207	212

[a] Linear; for *trans* bent $HCCF^+$,frequencies (cm^{-1}): ν_1 (A′) = 3377, ν_2 (A′) = 2061, ν_3 (A′) = 746, ν_4 (A′) = 719, ν_5 (A′) = 233, ν_6 (A″) = 720.
[b] HCCCl [41], HCCBr [46], HCCI [46].

The calculated and observed vibrational frequencies for the ground state and first excited state of $HCCX^+$ (X and A states, respectively) are listed in Tables 6 and 7. Experimentally, the HCCCl, HCCBr and HCCI cations are generated by electron impact in a supersonically cooled jet and the vibrational frequencies are obtained from the emission spectra. No experimental data is available for HCCF, presumably because the A state of $HCCF^+$ is not emissive. Spin-orbit coupling, vibrational resonances and Renner-Teller effects make the analysis of these spectra very challenging [48,49]. For the X state of $HCCX^+$, vibrational frequencies have been calculated with both the CCSD and EOMCC-IP approaches. The agreement between the two sets of calculated frequencies is quite good, differences ranging from −3 cm^{-1} to 32 cm^{-1} with a mean absolute deviation of 13 cm^{-1}. The CC triple bond stretching frequencies calculated with EOMCCSD-IP are systematically 15–32 cm^{-1} higher than with CCSD. This is because the CC bond lengths are 0.007 Å shorter with EOMCCSD-IP, possibly reflecting the greater difficulty in treating the electron correlation in the triple bond. The CX stretching frequencies calculated with both methods agree very well with the observed frequencies.

The frequencies for the A states of $HCCX^+$ can be computed with EOMCCSD-IP but not with conventional CCSD. The availability of experimental vibration frequencies for the A states is more limited than for the X state. The differences between calculated and observed frequencies for CC and CX stretch are a bit larger for $HCCI^+$ than for $HCCBr^+$ and $HCCCl^+$. The largest change in frequency and in geometry on going from the X state to the A state is in the C-X stretch. The calculated and experimental CX stretching frequencies for the A state are lower than for the X state, reflecting the longer CX bond in the A state. This effect increases as the halogen is changed from I to Br to Cl. Differences between the X and A states in the C–I bond length and C–I stretching frequency are key factors that determine the decay time for coherence and charge migration in HCCI [4,10–16].

The calculated and experimental frequencies are compared in Fig. 2. Overall, the agreement between the calculated and observed frequencies is very good. A linear least-squares fit with zero intercept yields ν_{calc} = 1.0505 ν_{exp} (R^2 = 0.9993, 61 data points). The calculated frequencies are about 5 % higher than observed primarily because anharmonicity corrections are not included in the calculations. Only a few vibrations deviate significantly from the linear correlation. These include the CC triple bond stretching mode in the X and A states of $HCCI^+$ and the CCH bending mode in the X state of $HCCI^+$. Potentially, this could be due to the larger spin-orbit coupling in $HCCX^+$ than in the other haloacetylene cations. The experimental splittings between the J = 3/2 and J = 1/2 spin orbit states of HCCX (X = Cl, Br and I) are 0.02, 0.13 and 0.40 eV, resp., for the X states and 0.05, 0.20 and 0.25 eV, resp., for the A states [43]. The CCH and CCX bending region, 200–700 cm^{-1}, shows a little more deviation than other regions. These bending modes are more

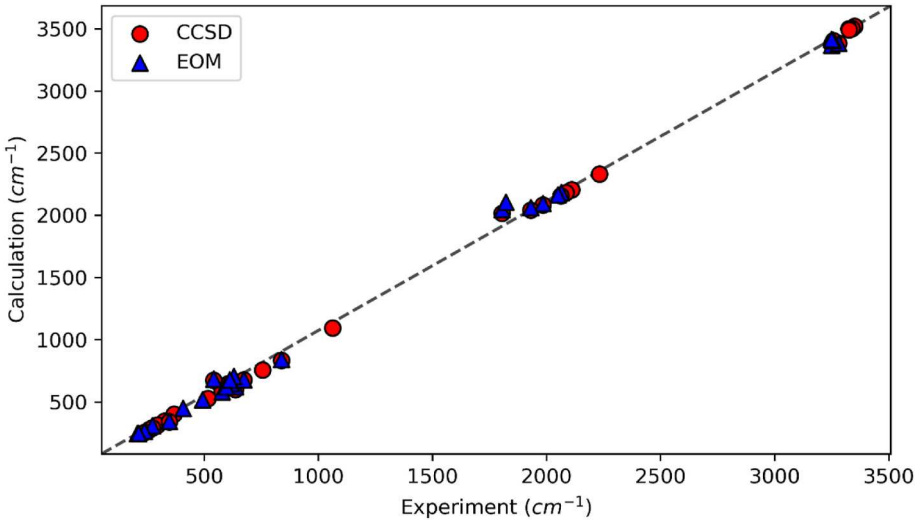

Fig. 2. Comparison of the calculated harmonic frequencies with the observed frequencies for neutral HCCX (X = F, Cl, Br and I) and X and A states of the HCCX cations (red circles: CCSD/cc-pVTZ.; blue triangles EOMCCSD-IP/cc-pVTZ; ν_{calc} = 1.0505 ν_{exp}, R^2 = 0.9993).

difficult to measure experimentally and are subject to Renner-Teller perturbations [48,49].

4. Conclusions

The coherent superposition of cation ground and excited states can produce charge migration on the femtosecond time scale. Modeling this charge migration requires information about the potential energy surfaces of the relevant cation states. CCSD can provide an accurate description of the ground state of the cation but cannot treat excited states with the same electronic symmetry as the ground state of the cation. CASSCF and CASPT2 are suitable methods but need to be customized for each molecule through the careful selection of an appropriate active space. The EOMCCSD-IP [20–23] is a convenient alternative. It is a reliable "black-box" method that can be used for the ground and excited states of the cation and is similar in quality to CCSD. Haloacetylene cations have been chosen as a test case. The superposition of the X and A states of $HCCX^+$ (X = F, Cl, Br and I) results in charge migration between the CC triple bond and the halogen π-type lone pair. The geometries, energies and vibrational frequencies have been calculated by CCSD/cc-pVTZ for neutral HCCX and the X state of $HCCX^+$ and by EOM CCSD-IP/cc-pVTZ for the X and A states of $HCCX^+$. The calculated vibrational frequencies for neutral HCCX and the X and A states of HCCX cation agree very well with available experimental data. Very good agreement is found for the calculated structures, ionization potentials and frequencies for the X state computed with CCSD and EOMCCSD-IP. This demonstrates that EOMCCSD-IP is a suitable method for modeling the ground and excited states for the HCCX cations.

CRediT authorship contribution statement

Andrew S. Durden: Investigation. **Marco Caricato:** Software. **H. Bernhard Schlegel:** Writing – review & editing, Writing – original draft, Investigation.

Declaration of competing interest

The authors declare that they have no known competing financial interests or personal relationships that could have appeared to influence the work reported in this paper.

Data availability

Data will be made available on request.

Acknowledgement

This work was supported by grants from the National Science Foundation to HBS (CHE1856437) and to MC (CHE2154452). ASD thanks WSU for supplemental support for a post-doctoral fellowship. The authors thank the Wayne State University computing grid for generous amounts of computer time.

References

[1] O. Smirnova, S. Patchkovskii, Y. Mairesse, N. Dudovich, M.Y. Ivanov, Strong-field control and spectroscopy of attosecond electron-hole dynamics in molecules, Proc. Natl. Acad. Sci. U. S. A. 106 (2009) 16556–16561, https://doi.org/10.1073/pnas.0907434106.

[2] E. Goulielmakis, Z.H. Loh, A. Wirth, R. Santra, N. Rohringer, V.S. Yakovlev, S. Zherebtsov, T. Pfeifer, A.M. Azzeer, M.F. Kling, et al., Real-time observation of valence electron motion, Nature 466 (2010) 739–744, https://doi.org/10.1038/nature09212.

[3] F. Calegari, D. Ayuso, A. Trabattoni, L. Belshaw, S. De Camillis, S. Anumula, F. Frassetto, L. Poletto, A. Palacios, P. Decleva, et al., Ultrafast electron dynamics in phenylalanine initiated by attosecond pulses, Science 346 (2014) 336–339, https://doi.org/10.1126/science.1254061.

[4] P.M. Kraus, B. Mignolet, D. Baykusheva, A. Rupenyan, L. Horný, E.F. Penka, G. Grassi, O.I. Tolstikhin, J. Schneider, F. Jensen, et al., Measurement and laser control of attosecond charge migration in ionized iodoacetylene, Science 350 (2015) 790–795, https://doi.org/10.1126/science.aab2160.

[5] N.V. Golubev, A.I. Kuleff, Control of charge migration in molecules by ultrashort laser pulses, Phys. Rev. A 91 (2015) 051401. https://doi.org/10.1103/PhysRevA.91.051401.

[6] M. Nisoli, P. Decleva, F. Calegari, A. Palacios, F. Martin, Attosecond electron dynamics in molecules, Chem. Rev. 117 (2017) 10760–10825, https://doi.org/10.1021/acs.chemrev.6b00453.

[7] H.J. Worner, C.A. Arrell, N. Banerji, A. Cannizzo, M. Chergui, A.K. Das, P. Hamm, U. Keller, P.M. Kraus, E. Liberatore, et al., Charge migration and charge transfer in molecular systems, Struct. Dyn.-US 4 (2017) 061508, https://doi.org/10.1063/1.4996505.

[8] D.T. Matselyukh, V. Despre, N.V. Golubev, A.I. Kuleff, H.J. Worner, Decoherence and revival in attosecond charge migration driven by non-adiabatic dynamics, Nat. Phys. 18 (2022) 1206–1213, https://doi.org/10.1038/s41567-022-01690-0.

[9] K. Mullerdethlefs, E.W. Schlag, High-resolution zero kinetic-energy (ZEKE) photoelectron-spectroscopy of molecular-systems, Annu. Rev. Phys. Chem. 42 (1991) 109–136, https://doi.org/10.1146/annurev.pc.42.100191.000545.

[10] H. Ding, D. Jia, J. Manz, Y.G. Yang, Reconstruction of the electronic flux during adiabatic attosecond charge migration in $HCCI^+$, Mol. Phys. 115 (2017) 1813–1825, https://doi.org/10.1080/00268976.2017.1287967.

[11] A.J. Jenkins, K.E. Spinlove, M. Vacher, G.A. Worth, M.A. Robb, The Ehrenfest method with fully quantum nuclear motion (Qu-Eh): application to charge migration in radical cations, J. Chem. Phys. 149 (2018) 094108, https://doi.org/10.1063/1.5038428.

[12] D. Jia, J. Manz, Y. Yang, De- and recoherence of charge migration in ionized iodoacetylene, J. Phys. Chem. Lett. 10 (2019) 4273–4277, https://doi.org/10.1021/acs.jpclett.9b01687.

[13] D. Jia, J. Manz, Y. Yang, Timing the recoherences of attosecond electronic charge migration by quantum control of femtosecond nuclear dynamics: a case study for $HCCI^+$, J. Chem. Phys. 151 (2019) 244306 https://doi.org/10.1063/1.5134665.

[14] D. Jia, Y. Yang, Systematic investigation of the reliability of the frozen nuclei approximation for short-pulse excitation: the example of $HCCI^+$, Front. Chem. 10 (2022) 857348. https://doi.org/10.3389/fchem.2022.857348.

[15] H.B. Schlegel, Charge migration in HCCI cations probed by strong field ionization: time-dependent configuration interaction and vibrational wavepacket simulations, J. Phys. Chem. A 127 (2023) 6040–6050, https://doi.org/10.1021/acs.jpca.3c02667.

[16] H.B. Schlegel, P. Hoerner, W. Li, Ionization of HCCI neutral and cations by strong laser fields simulated with time dependent configuration interaction, Front. Chem. 10 (2022) 866137, https://doi.org/10.3389/fchem.2022.866137.

[17] A.S. Folorunso, A. Bruner, F. Mauger, K.A. Hamer, S. Hernandez, R.R. Jones, L. F. DiMauro, M.B. Gaarde, K.J. Schafer, K. Lopata, Molecular modes of attosecond charge migration, Phys. Rev. Lett. 126 (2021) 133002. https://doi.org/10.1103/PhysRevLett.126.133002.

[18] K.A. Hamer, A.S. Folorunso, K. Lopata, K.J. Schafer, M.B. Gaarde, F. Mauger, Tracking charge migration with frequency-matched strobo-spectroscopy, J. Phys. Chem. A 128 (2024) 20–27, https://doi.org/10.1021/acs.jpca.3c04234.

[19] Y. Meng, H.H. Wang, Y.C. Zhang, Y.G. Yang, Ultrafast charge migration in ionized iodo-alkyne chain $I(CC)_nH^+$, AIP Adv. 13 (2023) https://doi.org/10.1063/5.0142214.

[20] D. Sinha, S. Mukhopadhyay, D. Mukherjee, A note on the direct calculation of excitation energies by quasi-degenerate MBPT and coupled-cluster theory, Chem. Phys. Lett. 129 (1986) 369–374, https://doi.org/10.1016/0009-2614(86)80361-X.

[21] S. Pal, M. Rittby, R.J. Bartlett, D. Sinha, D. Mukherjee, Multireference coupled-cluster methods using an incomplete model space: application to ionization potentials and excitation energies of formaldehyde, Chem. Phys. Lett. 137 (1987) 273–278, https://doi.org/10.1016/0009-2614(87)80218-X.

[22] M. Nooijen, J.G. Snijders, Coupled-cluster green-function method - working equations and applications, Int. J. Quantum Chem. 48 (1993) 15–48, https://doi.org/10.1002/qua.560480103.

[23] J.F. Stanton, J. Gauss, Analytic energy derivatives for ionized states described by the equation-of-motion coupled-cluster method, J. Chem. Phys. 101 (1994) 8938–8944, https://doi.org/10.1063/1.468022.

[24] R.J. Bartlett, M. Musiał, Coupled-cluster theory in quantum chemistry, Rev. Mod. Phys. 79 (2007) 291–352, https://doi.org/10.1103/RevModPhys.79.291.

[25] A.I. Krylov, Equation-of-motion coupled-cluster methods for open-shell and electronically excited species: the hitchhiker's guide to Fock space, Annu. Rev. Phys. Chem. 59 (2008) 433–462, https://doi.org/10.1146/annurev.physchem.59.032607.093602.

[26] R.J. Bartlett, Perspective on coupled-cluster theory. the evolution toward simplicity in quantum chemistry, Phys. Chem. Chem. Phys. 26 (2024) 8013–8037, https://doi.org/10.1039/D3CP03853J.

[27] P. Hoerner, H.B. Schlegel, Angular dependence of strong field ionization of haloacetylenes, HCCX (X = F, Cl, Br, I) using time-dependent configuration interaction with an absorbing potential, J. Phys. Chem. C 122 (2018) 13751–13757, https://doi.org/10.1021/acs.jpcc.8b00619.

[28] M.J. Frisch, G.W. Trucks, G. Scalmani, J.R. Cheeseman, X. Li, J. Bloino, B. G. Janesko, A.V. Marenich, J. Zheng, F. Lipparini, A.J. Jenkins, A. Liu, H. Liu, H. B. Schlegel, G.E. Scuseria, M.A. Robb, V. Barone, G.A. Petersson, H. Nakatsuji, B. Mennucci, C. Adamo, N. Rega, M. Caricato, H.P. Haratchian, J.V. Ortiz, F. Pawlowski, A.F. Izmaylov, H. Hu, C. Liao, J.L. Sonnenberg, D. Williams-Young, F. Ding, R. Gomperts, F. Egidi, J. Goings, B. Peng, A. Petrone, T. Henderson, D. Ranasinghe, V.G. Zakrzewski, J. Gao, G. Zheng, W. Liang, M. Hada, M. Ehara, K. Toyota, R. Fukuda, J. Hasegawa, M. Ishida, T. Nakajima, Y. Honda, O. Kitao, H. Nakai, T. Vreven, K. Throssell, J.J.A. Montgomery, J.E. Peralta, F. Ogliaro, M.

J. Bearpark, J.J. Heyd, E.N. Brothers, K.N. Kudin, V.N. Staroverov, T.A. Keith, R. Kobayashi, J. Normand, K. Raghavachari, A.P. Rendell, J.C. Burant, S.S. Iyengar, M. Cossi, J.M. Millam, M. Klene, R. Cammi, R.L. Martin, O. Farkas, J.B. Foresman, D.J. Fox, *Gaussian Development Version, Revision J.28+*. Wallingford CT, 2024.

[29] T.H. Dunning, Gaussian-basis sets for use in correlated molecular calculations .1. The atoms boron through neon and hydrogen, J. Chem. Phys. 90 (1989) 1007–1023, https://doi.org/10.1063/1.456153.

[30] D.E. Woon, Jr.T.H. Dunning, Gaussian basis sets for use in correlated molecular calculations. III. The atoms aluminum through argon, J. Chem. Phys. 98 (1993) 1358–1371, https://doi.org/10.1063/1.464303.

[31] K.A. Peterson, B.C. Shepler, D. Figgen, H. Stoll, On the spectroscopic and thermochemical properties of ClO, BrO, IO, and their anions, J. Phys. Chem. A 110 (2006) 13877–13883, https://doi.org/10.1021/jp065887l.

[32] K.A. Peterson, D. Figgen, E. Goll, H. Stoll, M. Dolg, Systematically convergent basis sets with relativistic pseudopotentials. II. Small-core pseudopotentials and correlation consistent basis sets for the post-d group 16–18 elements, J. Chem. Phys. 119 (2003) 11113–11123, https://doi.org/10.1063/1.1622924.

[33] J.V. Ortiz, Electron propagator theory: an approach to prediction and interpretation in quantum chemistry, WIREs Computational Molecular Science 3 (2013) 123–142, https://doi.org/10.1002/wcms.1116.

[34] R. Fletcher, M.J.D. Powell, A rapidly convergent descent method for minimization, Comput. J. 6 (1963) 163–168, https://doi.org/10.1093/comjnl/6.2.163.

[35] A.F. Borro, I.M. Mills, A. Mose, Overtone spectra and anharmonic resonances in haloacetylenes, Chem. Phys. 190 (1995) 363–371, https://doi.org/10.1016/0301-0104(94)00351-a.

[36] M. Leguennec, G. Wlodarczak, J. Demaison, H. Burger, O. Polanz, The millimeter-wave spectrum and structure of chloroacetylene, J. Mol. Spectrosc. 158 (1993) 357–362, https://doi.org/10.1006/jmsp.1993.1080.

[37] H. Jones, J. Sheridan, O.L. Stiefvater, Microwave-spectrum of bromoacetylene - r_s-structure, dipole-moment, quadrupole coupling-constants and excited vibration states, Z. Naturfor. 32 (1977) 866–875.

[38] U. Andresen, N. Heineking, H. Dreizler, Molecular-structure of iodoacetylene, J. Mol. Spectrosc. 137 (1989) 296–299, https://doi.org/10.1016/0022-2852(89)90173-2.

[39] D. Khiri, M. Hochlaf, G. Chambaud, Energetic diagrams and structural properties of monohaloacetylenes HC≡CX (X = F, Cl, Br), J. Phys. Chem. A 120 (2016) 5985–5992, https://doi.org/10.1021/acs.jpca.6b04504.

[40] E. Heilbronner, K.A. Muszkat, J. Schaublin, 6. An estimate of the interatomic distances in monohaloacetylene radical cations from photoelectron-spectroscopic data, Helv. Chim. Acta 54 (1971) 58–76.

[41] M.A. King, J.P. Maier, M. Ochsner, Laser-excitation spectra of the chloroacetylene and deuterochloroacetylene cations, $ClCCH^+$ and $ClCCD^+$, J. Chem. Phys. 83 (1985) 3181–3187, https://doi.org/10.1063/1.449175.

[42] J.P. Maier, M. Ochsner, The A-2-PI-3/2 -X-2-PI-3/2 laser-excitation spectra of iodoacetylene and deuteroiodoacetylene cations, J. Chem. Soc. Farad. Trans. 81 (1985) 1587–1598, https://doi.org/10.1039/f29858101587.

[43] M. Allan, E. Klosterjensen, J.P. Maier, Emission-spectra of Cl-C≡C-H^+,Br-C≡C-H^+ and I-C≡C-H^+ radical cations - alpha-2pi- chi-2pi band systems and decay of alpha-2pi states, J. Chem. Soc. Farad. Trans. 73 (1977) 1406–1416, https://doi.org/10.1039/f29777301406.

[44] G. Bieri, A. Schmelzer, L. Asbrink, M. Jonsson, Some comments on the perfluoroeffect .4. Fluorine and the fluoroderivatives of acetylene and diacetylene studied by 30.4 nm He(ii) photoelectron-spectroscopy, Chem. Phys. 49 (1980) 213–224, https://doi.org/10.1016/0301-0104(80)85258-x.

[45] G.R. Hunt, M.K. Wilson, Infrared spectra and potential constants of some monohaloacetylenes, J. Chem. Phys. 34 (1961) 1301–1308, https://doi.org/10.1063/1.1731736.

[46] J. Fulara, D. Klapstein, R. Kuhn, J.P. Maier, Emission-spectra of supersonically cooled haloacetylene cations - BrC≡C-H(D)$^+$, I-C≡C-H(D)$^+$, J. Phys. Chem. 90 (1986) 2061–2067, https://doi.org/10.1021/j100401a018.

[47] J. Lummila, O. Vaittinen, P. Jungner, L. Halonen, A.M. Tolonen, High-resolution FTIR and photoacoustic overtone spectrum of HCCl, J. Mol. Spectrosc. 185 (1997) 296–303, https://doi.org/10.1006/jmsp.1997.7426.

[48] B. Gans, G. Grassi, F. Merkt, Spin-orbit and vibronic coupling in the ionic ground state of iodoacetylene from a rotationally resolved photoelectron spectrum, J. Phys. Chem. A 117 (2013) 9353–9362, https://doi.org/10.1021/jp310241d.

[49] W. Sun, Z.Y. Dai, J. Wang, Y.X. Mo, The Renner-Teller effect in $HCCCl^+$ ($X\ ^2\Pi$) studied by zero-kinetic energy photoelectron spectroscopy and *ab initio* calculations, J. Chem. Phys. 142 (2015) 194304. https://doi.org/10.1063/1.4919953.